View metadata, citation and similar papers at core.ac.uk
brought to you by CORE
provided by idUS. Depósito de Investigación Universidad de Sevilla

PHYSICAL REVIEW E **91**, 012905 (2015)

Soliton stability criterion for generalized nonlinear Schrödinger equations

Niurka R. Quintero,[1,*] Franz G. Mertens,[2] and A. R. Bishop[3]
[1]*IMUS and Departamento de Física Aplicada I, E.S.P., Universidad de Sevilla, Virgen de África 7, E-41011 Sevilla, Spain*
[2]*Physikalisches Institut, Universität Bayreuth, 95440 Bayreuth, Germany*
[3]*Los Alamos National Laboratory, Los Alamos, New Mexico 87545, USA*
(Received 26 June 2014; published 9 January 2015)

A stability criterion for solitons of the driven nonlinear Schrödinger equation (NLSE) has been conjectured. The criterion states that $p'(v) < 0$ is a sufficient condition for instability, while $p'(v) > 0$ is a necessary condition for stability; here, v is the soliton velocity and $p = P/N$, where P and N are the soliton momentum and norm, respectively. To date, the curve $p(v)$ was calculated approximately by a collective coordinate theory, and the criterion was confirmed by simulations. The goal of this paper is to calculate $p(v)$ exactly for several classes and cases of the generalized NLSE: a soliton moving in a real potential, in particular a time-dependent ramp potential, and a time-dependent confining quadratic potential, where the nonlinearity in the NLSE also has a time-dependent coefficient. Moreover, we investigate a logarithmic and a cubic NLSE with a time-independent quadratic potential well. In the latter case, there is a bisoliton solution that consists of two solitons with asymmetric shapes, forming a bound state in which the shapes and the separation distance oscillate. Finally, we consider a cubic NLSE with parametric driving. In all cases, the $p(v)$ curve is calculated either analytically or numerically, and the stability criterion is confirmed.

DOI: 10.1103/PhysRevE.91.012905 PACS number(s): 05.45.Yv, 05.60.Cd

I. INTRODUCTION

The stability criteria for the homogeneous (translationally invariant) nonlinear Schrödinger equation (NLSE) in $1+1$ dimensions that are available in the literature are restricted to (a) bright solitons, i.e., solutions decaying to zero at the spatial infinities, with time dependencies of the form $e^{i\Lambda t}$ (and those reducible to this form by a Galileian transformation); and (b) traveling dark solitons (solutions approaching nonzero constant values as $x \to \pm\infty$). The criteria are insensitive to the particular form of the nonlinearity as long as it is conservative and U(1) invariant, i.e., as long as the NLSE does not include any driving or damping terms.

In the case of the bright solitons of the form $u(x,t) = u_s(x)e^{i\Lambda t}$, the Vakhitov-Kolokolov criterion states that if the corresponding energy Hessian has only one negative eigenvalue, then the soliton is stable if the variation of the norm $dN/d\Lambda > 0$ and unstable otherwise [1–3]. Here, $N = \int |u|^2 dx$ is denoted as the norm, or as the number of particles contained in the soliton.

There is a similar criterion [4–7] for dark solitons of the form $u(x,t) = u_s(x - vt)$, with $|u_s|^2 \to \rho_0$ as $x \to \pm\infty$. The dark soliton traveling at the constant velocity v is stable if $dP/dv < 0$, and unstable otherwise; P is a renormalized field momentum. A rigorous proof of the stability criterion was given by Lin [8]. A similar stability criterion, which also uses a renormalized momentum, was established in Ref. [9] for dark and bright solitons of the *undriven* cubic-quintic NLSE.

Some parts of the stability analysis of the traveling dark solitons [7] can be carried over to the case of traveling bright solitons of the NLSE with a *driving* term. Namely, a linear stability analysis shows [10] that a pair of eigenvalues crosses from the imaginary to the real axis at the value v_0 where $P'(v) = dP/dv = 0$. The sign of $P'(v)$ required for stability depends on the type of soliton; some classes require $P' < 0$, whereas other classes are stable when $P' > 0$. Each point of the curve $P(v)$ represents a soliton traveling at a particular constant velocity v; therefore, the curve is a characteristic of the whole family of solitons. The values of v_0 where $P' = 0$ break the family into parts with different stability properties. The disadvantage of this stability criterion is that one always has to solve *numerically* a linear eigenvalue problem before a prediction about the stability of solitons of a particular type of NLSE can be made.

In recent years, a very different type of stability criterion was conjectured by us and confirmed by numerical simulations [11,12]. For the NLSE,

$$iu_t + u_{xx} + 2|u|^2u + \delta u = R, \tag{1}$$

with a spatiotemporal external driving of the form

$$R = re^{-iK(t)x}, \tag{2}$$

a collective coordinate (CC) theory was developed. This theory uses the one-soliton solution of the unperturbed NLSE [Eq. (1) with $R \equiv 0$] in order to make an ansatz for $u(x,t)$ with four collective coordinates: soliton position $q(t)$, amplitude $\beta(t)$, phase $\phi(t)$, and normalized momentum $p(t) = P(t)/N(t)$. The momentum $P(t)$ of the field $u(x,t)$ is identical to the momentum conjugate to the soliton position $q(t)$. In this approach, the Lagrangian of the driven NLS Eq. (1) is a function of the collective coordinates and their time derivatives. The Lagrange equations form a set of coupled nonlinear ordinary differential equations (CC equations) that can be solved analytically or numerically (see below). The solutions for $p(t)$ and the soliton velocity $v(t) = \dot{q}(t)$ form a parametric representation of the so-called "stability curve" $p(v)$, which is obtained by elimination of the time t. This means that each solution of the CC equations has its own, individual $p(v)$ curve, the whole of which is traced in time.

*niurka@us.es

 ©2015 American Physical Society

The conjectured criterion [11,12] states that

$$dp/dv < 0 \tag{3}$$

is a *sufficient* condition for *instability* of the soliton, and

$$dp/dv > 0 \tag{4}$$

is a *necessary* condition for *stability*. Thus the slope of the curve $p(v)$ predicts whether the corresponding soliton is stable or not.

Note that this is quite different from the above criterion [10] where the curve $P(v)$ represents a family of solitons in which each soliton travels at a particular *constant* velocity. Thus this criterion cannot be applied to solitons with time-dependent velocity. Also note that the *renormalized* momentum that is used in Refs. [7–10] differs conceptually from the normalized momentum $p(t) = P(t)/N(t)$, which is used in the conjectured criterion Eqs. (3) and (4).

The conjectured criterion was empirically confirmed by numerical simulations for the NLS Eq. (1) in the following cases:

(i) Time-independent, spatially periodic driving of the form $r\exp(-iKx)$; here, the soliton displays periodic oscillations of the velocity, momentum, amplitude, and phase. Although the driving force has zero spatial average, the soliton's net motion is *unidirectional*. The initial conditions (ICs) determine whether the soliton is stable or not [11].

(ii) Spatiotemporal driving of the form $R = r\exp[-iK(t)x]$ with harmonic $K(t)$. In this case, the solutions of the CC equations exhibit oscillations with three very different frequencies [12]: an intrinsic frequency ω_i, the frequency ω of the harmonic function $K(t)$, and a very low frequency ω_l. Stable solitons are predicted and confirmed by simulations only when the intrinsic oscillations are suppressed by choosing an IC with $\beta_0 = \sqrt{-\delta}$. When the damping term $-i\alpha u(x,t)$ with $\alpha > 0$ is included in the right-hand side of the NLS Eq. (1), the CC dynamics simplifies: both the ω_i and ω_l oscillations are damped out after a transient time $1/\alpha$. After this transient, all CC oscillations become locked to the driving frequency ω. The stability curve $p(v)$ does not have any sections with a negative slope, and the stability of the soliton is indeed confirmed by simulations [12].

(iii) Driving of the same form as in case (ii), but with a biharmonic force [12]. Including the same damping term as in case (ii), a soliton ratchet can be obtained. However, in order to obtain stable solitons, the damping parameter α must be in a certain range, and a special IC must be chosen that yields a straight stability curve with a positive slope. The soliton stability is confirmed by simulations for the NLSE [12].

(iv) Instead of the cubic NLS Eq. (1), an NLSE with the nonlinearity $g|u|^{2\kappa}u$ was investigated [13], with positive coupling constant g, arbitrary positive nonlinearity exponent κ, and the same driving as in case (i). For the unperturbed case ($R \equiv 0$), there exist exact one-soliton solutions [13] that were used as the ansatz for a CC theory. The resulting CC equations were solved analytically in the cases of stationary solutions and small oscillations about them. Otherwise, the equations were solved numerically for the case $\kappa = 1/2$. The solutions describe oscillating solitons, and the criterion Eq. (3) makes predictions for which IC unstable solitons are expected, which is confirmed by simulations [13].

(v) In addition to the nonparametric (external) drivings in cases (i)–(iv), the case of parametric driving has also been investigated, choosing $R = re^{2iKx}u^*(x,t)$ with time-independent K [14]. In this case, the four CC equations can be reduced to two equations, and the stability curve can be obtained analytically. The stability or instability of the solitons, depending on the IC, is confirmed by simulations.

In the above five cases, the stability curve was computed or calculated by using the parametric representation $p(t), v(t)$ of the curve. Here $p(t)$ and $v(t)$ were obtained from the solutions of the CC equations for each of the cases.

The CC theories naturally are approximations because they have only a few degrees of freedom, whereas the NLSE are partial differential equations (PDEs), which have infinitely many degrees of freedom. The main goal of this paper is to calculate *exactly* the stability curve, without using collective variables.

In Sec. II, we consider a generalized NLSE (GNLSE) with arbitrary nonlinearity $G(|u|)$ and arbitrary driving $R[u(x,t);x,t]$, and we derive an expression for $p(t)$ that contains two integrals that cannot be evaluated in a general way. The first integral vanishes in most cases, namely when the soliton shape is symmetric. The second integral contains the driving R. In Secs. III and IV, we investigate several classes of GNLSE for which the above integrals can be calculated. In particular, we show that the second integral vanishes when the soliton moves in a real potential $V(x)$, i.e., $R = V(x)u(x,t)$.

In the case of a cubic NLSE with the ramp potential $V(x) = 2\alpha x$, an exact soliton was obtained by a direct method [15]. We generalize this for the nonlinearity $G = |u|^{2\kappa}$ and the time-dependent ramp potential $V(x,t) = f(t)(2\alpha x - \delta)$. The stability curve is a straight line with positive slope, so the stability criterion (4) is fulfilled (Sec. III).

In Sec. III, we also consider a GNLSE with a time-dependent confining *quadratic* potential $V(x,t) = k(t)x^2$, where the nonlinearity has the form $g(t)|u|^2u$. When a certain integrability condition holds [16,17], an exact one-soliton solution can be obtained that allows the exact calculation of the stability curve, which is a straight line with positive slope. Thus, the criterion Eq. (4) is fulfilled.

The special case $k(t) = g(t) \equiv 1$ is identical with the cubic NLSE with a time-independent confining quadratic potential. However, here the integrability condition of Refs. [16,17] is *not* fulfilled, thus the self-similar transformation method [17] cannot be applied. To the best of our knowledge, an exact, analytical one-soliton solution is not known in the literature. However, such a solution was obtained for the *logarithmic* NLSE [18]. Here intrinsic anharmonic oscillations of the soliton are coupled to the harmonic oscillations of the soliton position. For this solution, we calculate the stability curve and find that the criterion (4) is again fulfilled (Sec. III).

The stability criteria in Eqs. (3) and (4) were conjectured and confirmed for *single* solitons with a symmetric shape [11,12]. In Sec. IV, we test whether the criteria also hold for *bisolitons* in a cubic NLSE with a parabolic potential well. Here two solitons with asymmetric shapes form a bound state in which their shapes and their separation distance oscillate. We observe this in numerical simulations, using an IC obtained by modifying a result for the case of a parabolic potential

barrier [19], where two asymmetric lumps move away from each other, become smaller, and vanish eventually.

Finally, in order to have examples for stability curves with negative slope, we take the parametric driving $R = re^{-2iKx}u^*(x,t)$ (Sec. V). We numerically integrate the NLS Eq. (5) with $G(|u|) = |u|^2$ and obtain $u(x,t)$. This is used to compute the normalized momentum $p(t) = P(t)/N(t)$, the soliton position $q(t) = N_1(t)/N(t)$, where N_1 is the first moment of the norm, and the velocity $\dot{q}(t) \equiv v(t)$. Then the time is eliminated to give the stability curve $p(v)$. Depending on the IC, the soliton can be stable or unstable.

II. SOLITONS WITH VANISHING BOUNDARY CONDITIONS

We consider the generalized NLSE

$$iu_t + \tfrac{1}{2}\gamma u_{xx} + 2G(|u|)u = R[u(x,t);x,t], \tag{5}$$

with a real positive parameter γ and a real function G, and we assume that an exact one-soliton solution exists, which is represented by

$$u(x,t) = u^{(s)}(x - q(t),t), \tag{6}$$

where $q(t)$ is the soliton position. The explicit time dependence means that the soliton shape may change during the time evolution [in cases (i)–(v) in the Introduction, the shape changes periodically].

We multiply the NLS Eq. (5) by u^* and the complex conjugate NLSE by u, subtract the two equations, and obtain

$$\frac{\partial \rho}{\partial t} + \frac{\partial j}{\partial x} = i(R^*u - \text{c.c.}), \tag{7}$$

with the norm density

$$\rho(x,t) = |u|^2 \tag{8}$$

and the momentum current density

$$j(x,t) = \frac{i}{2}(uu_x^* - \text{c.c.}). \tag{9}$$

We multiply Eq. (7) by x, integrate over all x, and obtain

$$\frac{dN_1}{dt} = \gamma P + \int_{-\infty}^{+\infty} dx\, ix(R^*u - \text{c.c.}). \tag{10}$$

Here the integrated term $xj|_{-\infty}^{+\infty}$ vanishes when we insert the soliton solution, because we assume that $u^{(s)}$ or $u_x^{(s)}$ vanishes stronger than $1/x$ for $x \to \pm\infty$,

$$N_1(t) = \int_{-\infty}^{+\infty} dx\, x|u(x,t)|^2, \tag{11}$$

is the first moment of the norm $N(t) = \int_{-\infty}^{+\infty} dx\, |u(x,t)|^2$, and

$$P(t) = \int_{-\infty}^{+\infty} dx\, j(x,t) \tag{12}$$

is the field momentum.

We now insert the soliton solution into $N(t)$ and $N_1(t)$, and we change variables by $x - q(t) = y$ and denote

$$u^{(s)}(x - q(t),t) = \tilde{u}(y,t). \tag{13}$$

We calculate

$$N(t) = \int_{-\infty}^{+\infty} dy|\tilde{u}|^2 = \tilde{N}(t), \tag{14}$$

$$N_1(t) = \int_{-\infty}^{+\infty} dy\, y\,|\tilde{u}|^2 + qN = \tilde{N}_1 + qN. \tag{15}$$

$\tilde{N}_1$ vanishes if the soliton shape $|\tilde{u}|^2$ is symmetric; this is the case for the five types of NLSEs presented in the Introduction. However, we keep $\tilde{N}_1$ because we will also consider the case of an asymmetric soliton. Equation (10) can be written as

$$P = \tilde{P} = \frac{1}{\gamma}\dot{q}N + \frac{1}{\gamma}q\dot{N} + \frac{1}{\gamma}\dot{\tilde{N}}_1 - \frac{i}{\gamma}\int_{-\infty}^{+\infty} dy(y+q)(\tilde{R}^*\tilde{u} - \text{c.c.}), \tag{16}$$

with $\tilde{R} = R[\tilde{u}(y,t); y + q, t]$. The second term on the right-hand side of Eq. (16) and the second part of the integral cancel, because the integration of Eq. (7) yields

$$\dot{N} = i\int_{-\infty}^{+\infty} dx(R^*u - \text{c.c.}) = i\int_{-\infty}^{+\infty} dy(\tilde{R}^*\tilde{u} - \text{c.c.}). \tag{17}$$

Finally, we divide Eq. (16) by N and obtain for the normalized momentum $p = P/N$

$$p(t) = \frac{1}{\gamma}\dot{q} + \frac{1}{\gamma}\frac{\dot{\tilde{N}}_1(t)}{N(t)} + \frac{1}{\gamma}F(t), \tag{18}$$

with

$$F(t) = -\frac{i}{N}\int_{-\infty}^{+\infty} dy\, y(\tilde{R}^*\tilde{u} - \text{c.c.}). \tag{19}$$

To obtain the stability curve $p(v)$ (see the Introduction), it is necessary to eliminate the time from the parametric representation $p(t)$, $v(t) = \dot{q}$ of the curve. That is, the inverse function $t(\dot{q})$ must be inserted in $F(t)$. Since the integral Eq. (19) cannot be performed for arbitrary R, in the following we choose R such that this integral can be evaluated.

III. SYMMETRIC SOLITON IN A POTENTIAL

We consider a soliton that moves in a real potential $V(x,t)$ that may also depend on time. This means that $R = V(x,t)u(x,t)$ and in Eq. (19) $\tilde{R}^*\tilde{u} - \text{c.c.} = \tilde{V}(y,t)|\tilde{u}|^2 - \text{c.c.} = 0$, i.e., $F(t)$ vanishes. If the soliton profile is symmetric, i.e., $\tilde{u}(y,t) = \tilde{u}(-y,t)$, $\tilde{N}_1(t)$ in Eq. (15) also vanishes and Eq. (18) yields the very simple result,

$$p(t) = \frac{1}{\gamma}\dot{q}(t). \tag{20}$$

The stability curve $p(v) = \frac{1}{\gamma}v$ is a straight line with slope $p'(v) = \frac{1}{\gamma} > 0$, and the necessary condition for stability, Eq. (4), is fulfilled.

To confirm this general result, we consider several classes and examples of GNLSEs. In all cases, $p(t)$ and $\dot{q}(t)$ can be calculated exactly.

The first class consists of the GNLSE (5) with the nonlinearity $G = |u(x,t)|^{2\kappa}$ with $\kappa > 0$ and a linear potential (ramp potential), i.e., $R = V(x,t)u(x,t) = f(t)(2\alpha x - \delta)u(x,t)$, with the real parameters δ and α. Compared to Ref. [15], we have included an arbitrary real function $f(t)$; moreover, Ref. [15] only considered the case $\kappa = 1$.

Using the ansatz

$$u(x,t) = A(x,t)e^{i\varphi(x,t)} \tag{21}$$

with real A and φ, we obtain

$$\frac{\partial}{\partial t}A^2 + \frac{\partial}{\partial x}(\gamma A^2\varphi_x) = 0, \tag{22}$$

$$\left(-\varphi_t - \frac{\gamma}{2}\varphi_x^2 + 2|A|^{2\kappa}\right)A + \frac{\gamma}{2}A_{xx} = f(t)(\delta - 2\alpha x)A. \tag{23}$$

We generalize the ansatz of Ref. [15] by assuming

$$A(x,t) = \tilde{A}\,\mathrm{sech}^{\tilde{\kappa}}\{\beta[x - q(t)]\}, \tag{24}$$

$$\varphi(x,t) = p(t)[x - q(t)] + \phi(t), \tag{25}$$

where β, $\tilde{A}$, and $\tilde{\kappa}$ are real constants. Inserting Eqs. (24) and (25) in Eq. (22), we obtain $\dot{q} = \gamma p(t)$ *for all* κ *and independent of* $f(t)$. This means that the stability curve $p(v) = \frac{1}{\gamma}v$ is always a straight line with positive slope.

Inserting Eqs. (24) and (25) in Eq. (23), we obtain a complicated ordinary differential equation (ODE) which simplifies considerably for $\tilde{\kappa} = 1/\kappa$ and

$$\tilde{A} = \left[\frac{\gamma}{2}\frac{\beta^2(\kappa+1)}{2\kappa^2}\right]^{1/(2\kappa)}. \tag{26}$$

The ODE is then solved by

$$p(t) = p_0 - 2\alpha\int_0^t f(\tau)d\tau, \tag{27}$$

$$q(t) = q_0 + \gamma\int_0^t p(\tau)d\tau, \tag{28}$$

$$\phi(t) = \phi_0 + \int_0^t\left[\frac{\gamma}{2}p^2 + \frac{\gamma}{2}\frac{\beta^2}{\kappa^2} + (\delta - 2\alpha q)f(\tau)\right]d\tau. \tag{29}$$

In the special case $f(t) \equiv 1$, we find

$$p(t) = p_0 - 2\alpha t, \tag{30}$$

$$q(t) = q_0 + \gamma p_0 t - \gamma\alpha t^2, \tag{31}$$

$$\phi(t) = \phi_0 + \left(\delta - 2\alpha q_0 + \frac{\gamma}{2}p_0^2 + \frac{\gamma}{2}\frac{\beta^2}{\kappa^2}\right)t - 2\alpha\gamma p_0 t^2 + \frac{4}{3}\alpha^2\gamma t^3. \tag{32}$$

For $\kappa = 1$, this agrees with the one-soliton solution of Ref. [15], where the N-soliton solution was obtained by using the inverse scattering theory (IST).

The second class of GNLSEs contains a quadratic potential, multiplied by a function $k(t)$, and a second function $g(t) > 0$ multiplying a cubic nonlinearity [17]:

$$iu_t + \tfrac{1}{2}u_{xx} + g(t)|u|^2u = k(t)x^2u. \tag{33}$$

For simplicity, we have set $\gamma = 1$. $k(t)$ and $g(t)$ are not arbitrary, because Eq. (33) can be converted by a modified Lens-type transformation, or a self-similar transformation [20–22], to the standard NLSE,

$$i\frac{\partial\Phi}{\partial T} + \frac{1}{2}\frac{\partial^2\Phi}{\partial X^2} + |\Phi|^2\Phi(X,T) = 0, \tag{34}$$

if an integrability condition holds [17],

$$g\ddot{g} - 2\dot{g}^2 - 2kg^2 = 0. \tag{35}$$

The same condition was obtained by IST in Ref. [16].

Solutions of Eq. (33) can be obtained from the well-known solutions of the standard NLSE by the transformation

$$u(x,t) = \sqrt{g(t)}\Phi(X,T)e^{-\frac{i}{2}\frac{\dot{g}}{g}x^2}, \tag{36}$$

with

$$X(x,t) = g(t)x, \qquad T = \int_0^t g^2(\tau)d\tau. \tag{37}$$

The one-soliton solution of Eq. (34) is

$$\Phi(X,T) = A_s\mathrm{sech}[A_s(X - X_0 - k_sT)]e^{i[k_sX + (A_s^2 - k_s^2)\frac{T}{2} + \phi_0]}, \tag{38}$$

where A_s, k_s, X_0, and ϕ_0 are arbitrary real constants, and in the following we set $X_0 = \phi_0 = 0$.

The one-soliton solution of Eq. (33) is then

$$u(x,t) = A_s\sqrt{g(t)}\mathrm{sech}\{A_s[X(x,t) - k_sT(t)]\}e^{i\psi}, \tag{39}$$

with

$$\psi(x,t) = k_sX(x,t) + \frac{1}{2}(A_s^2 - k_s^2)T(t) - \frac{1}{2}\frac{\dot{g}}{g}x^2. \tag{40}$$

The soliton has the amplitude $A_s\sqrt{g}$ and width $1/(A_sg)$, therefore the norm

$$N = \int_{-\infty}^{+\infty}dx|u|^2 = 2A_s \tag{41}$$

is time-independent. The soliton profile is symmetric with respect to the soliton position $q(t)$, which is defined as the position of the maximum of $|u|^2$. This position is obtained from $X(q,t) = k_sT(t)$, which yields $q(t) = k_sT(t)/g(t)$ using Eq. (37).

For the stability curve, we need the velocity $\dot{q} = k_s(g - T\dot{g}/g^2)$ and the momentum. The momentum current density Eq. (9) is obtained as

$$j(x,t) = A_s^2g(t)\mathrm{sech}^2(y)(k_sg - x\dot{g}/g), \tag{42}$$

with $y = A_s(gx - k_sT)$. The momentum Eq. (12) is $P = 2A_sk_s(g - T\dot{g}/g^2) = 2A_s\dot{q}$. Using Eq. (41), we finally obtain the normalized momentum $p(t) = P(t)/N = \dot{q}$. The stability curve $p(v) = v$ is a straight line with slope 1. Thus we have shown that the necessary stability condition $dp/dv > 0$ is fulfilled for the above class of GNLSE with arbitrary functions $k(t)$ and $g(t)$, provided that they fulfill the integrability condition Eq. (35).

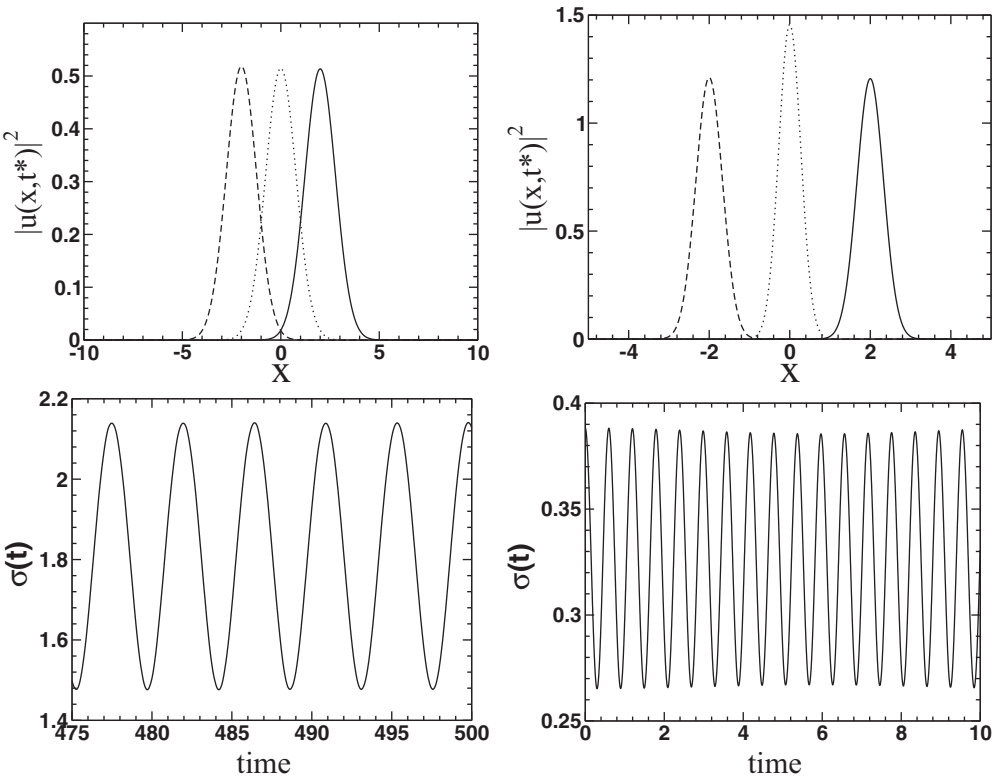

FIG. 1. Simulations of the logarithmic NLSE with a harmonic potential well. Left and right panels: $\omega = 0.05$, $\lambda = 1$ and $\omega = 5$, $\lambda = 1$, respectively. Upper panels: soliton profiles for different times: $t^* = 0$ (solid line), $t^* = T/4$ (dotted line), and $t^* = T/2$ (dashed line). Lower panels: soliton width $\sigma(t)$ oscillates with frequency 1.4078 (left panel) and 10.53 (right panel).

However, this condition is *not* fulfilled for the simplest case $k(t) \equiv 1$ and $g(t) \equiv 1$. Here, to our knowledge, an exact, analytical one-soliton solution is not known in the literature. Instead of the cubic nonlinearity, we therefore consider the logarithmic NLS Eq. (5) with $G = \frac{1}{2}\lambda^2 \ln|u|$, $\gamma = 1$, and $R = V(x)u(x,t)$, where $V = \frac{1}{2}\omega^2 x^2$ is a quadratic potential well [18]. Writing $u(x,t)$ as in Eq. (21), the soliton envelope is a Gaussian,

$$A(x,t) = \frac{1}{\pi^{1/4}\sigma^{1/2}} \exp\left[-\frac{(x-q)^2}{2\sigma^2}\right], \tag{43}$$

where the soliton position $q(t)$ performs harmonic oscillations with frequency ω. The phase of the soliton is

$$\varphi(x,t) = x\dot{q} + \frac{\dot{\sigma}}{\sigma}\left(\frac{1}{2}x^2 - xq\right) + B(t), \tag{44}$$

where $B(t)$ is an integration constant. The soliton width $\sigma(t)$ fulfills the nonlinear oscillator equation

$$\ddot{\sigma} + \omega^2\sigma - \frac{1}{\sigma^3} + \frac{\lambda^2}{\sigma} = 0. \tag{45}$$

We remark that in Ref. [18] there is a factor 2 at the term σ^{-3} and a factor $\dot{\sigma}$ multiplying the whole left-hand side of Eq. (45). Due to the factor $\dot{\sigma}$, solutions with *arbitrary* constant width would be admitted. However, this is not confirmed by our simulations, which confirm Eq. (45), which has only one solution with constant width,

$$\bar{\sigma}^2 = \frac{1}{2\omega^2}(\sqrt{\lambda^4 + 4\omega^2} - \lambda^2). \tag{46}$$

All other solutions are anharmonic oscillations around $\bar{\sigma}$.

For small amplitude, the oscillations are harmonic with frequency

$$\nu^2 = \omega^2 + \frac{3}{\bar{\sigma}^4} - \frac{\lambda^2}{\bar{\sigma}^2}. \tag{47}$$

The appearance of ω^2 in Eqs. (45)–(47) shows that the intrinsic oscillations of the width are coupled to the harmonic oscillations of the soliton in the quadratic well.

For the discussion of Eq. (47), we distinguish two regimes:

(i) For $\omega \ll \lambda^2/2$, the potential is weak compared to the nonlinearity. Here the average soliton width $\bar{\sigma}$ is much smaller than the characteristic length $l = 1/\omega$ of the potential. The frequency

$$\nu^2 = 2\lambda^4\left(1 + \frac{\omega^2}{2\lambda^4}\right) \tag{48}$$

shows that the intrinsic oscillations are only weakly coupled to the translational motion.

For $\omega = 0.05$ and $\lambda = 1$, we have $\nu = 1.415$, which agrees very well with the simulation result $\nu = 1.408$; see Fig. 1 (left panels). This rules out the above factor 2 at the term σ^{-3} in Ref. [18].

(ii) For $\omega \gg \lambda^2/2$, we have

$$\nu^2 = 4\omega^2\left(1 + \frac{\lambda^2}{2\omega}\right). \tag{49}$$

Here $\bar{\sigma} = O(l)$ and $\nu \approx 2\omega$, which means that the intrinsic oscillations are strongly coupled to the translational motion.

For $\omega = 5$ and $\lambda = 1$, $v = 10.49$, which agrees well with 10.53; see Fig. 1 (right panels).

Finally, we calculate the stability curve. The momentum current density Eq. (9) results in

$$j(x,t) = \frac{1}{\sqrt{\pi\sigma^2}} \exp[-(x-q)^2/\sigma^2][\sigma\dot{q} + (x-q)\dot{\sigma}]. \quad (50)$$

The integration over x yields $P(t) = \dot{q}$ and the same for $p(t) = P(t)/N$, because $N = 1$. This means that the necessary condition for stability is fulfilled.

IV. ASYMMETRIC SOLITONS

In cases (i)–(v) in the Introduction, and in all the cases of GNLSEs in Sec. III, the soliton profile is always symmetric with respect to the center of mass. If the profile is not symmetric, the term with $\dot{\tilde{N}}_1(t)$ in Eq. (18) does not vanish and therefore the stability curve $p(v)$ cannot be a straight line and the slope of the curve could be negative somewhere.

A solution with two asymmetric lumps was obtained by an IST by Balakrishnan [19] who investigated the GNLSE,

$$iu_t + \tfrac{1}{2}u_{xx} + 2|u|^2u = 2V(x)u, \quad (51)$$

with the quadratic potential

$$V(x) = \tfrac{1}{4}\mu\lambda x^2 + \mu\lambda_0 x + \mu_0, \quad (52)$$

with arbitrary real constants $\lambda, \mu; \lambda_0, \mu_0$. In Ref. [19], only the case of a parabolic potential *barrier* ($\mu\lambda < 0, \lambda_0 = 0, \mu_0 = 0$) was explicitly considered, and it resulted in the solution

$$u(x,t) = \sqrt{\frac{2c^*}{c}}\eta(t)\, x\, \mathrm{sech}\left[\lambda\eta(t)x^2 + \ln\frac{2\eta(t)}{|c|}\right] e^{-i\lambda\xi(t)x^2}. \quad (53)$$

Here $\xi(t)$ and $\eta(t)$ are the real and imaginary parts of the complex time-dependent eigenvalue in the IST. $u(x,t)$ in Eq. (53) is antisymmetric in x, the envelope comprising two lumps at the positions $q(t)$ and $-q(t)$ on the positive and negative x axis, respectively. The two lumps move away from each other, become smaller and smaller, and eventually vanish.

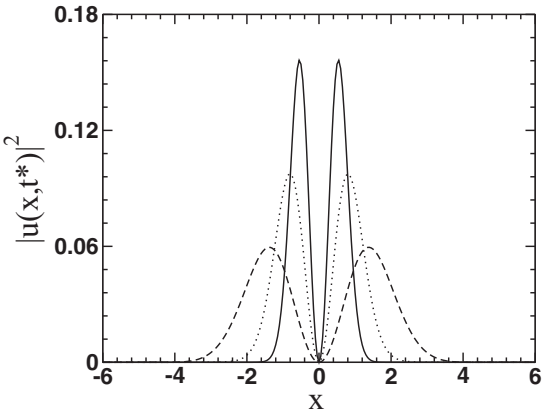

FIG. 2. Profile $|u(x,t^*)|^2$ of a bisoliton in a parabolic potential well for different times in units of $T = \pi$ (solid line $t^* = 0$, dotted line $t^* = 2T$, dashed line $t^* = 6T$). Simulations of Eq. (51) with the potential (52), with $\lambda_0 = \mu_0 = 0, \mu = 1$, and $\lambda = 2$. IC: Eq. (53) with $\eta(0) = 1, \xi(0) = 0, c = 1$.

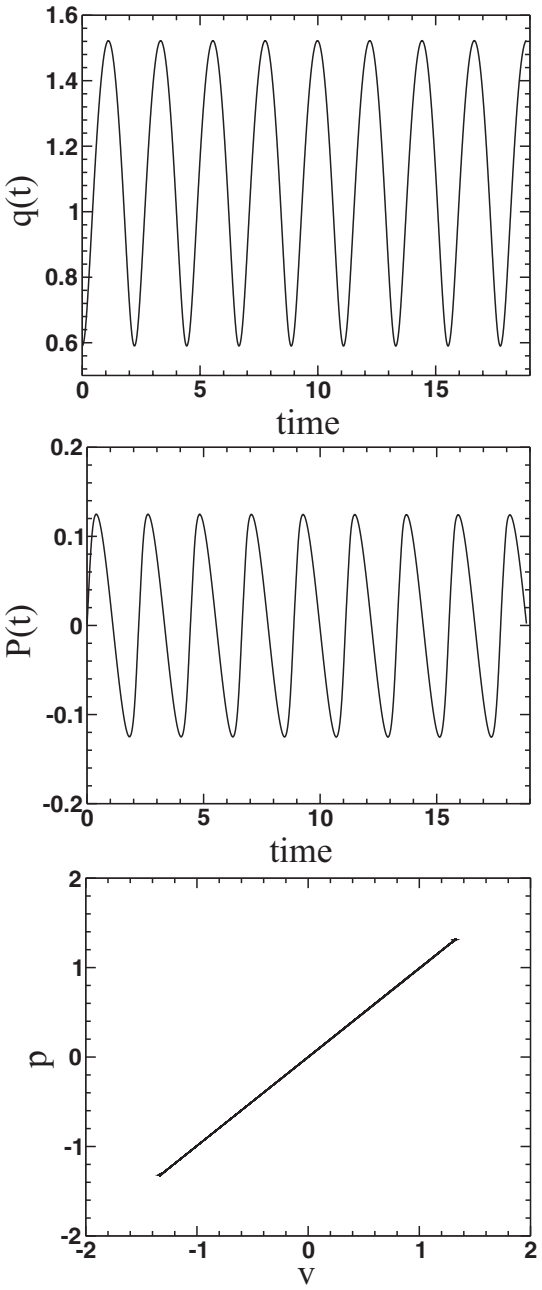

FIG. 3. Position $q(t)$ and momentum $P(t)$ of the right soliton of the bisoliton in Fig. 2. The slope of the $p(v)$ curve is 0.992 with a correlation coefficient 0.999 98.

We consider the case of a parabolic potential *well* ($\mu\lambda > 0$, $\lambda_0 = \mu_0 = 0$) and take $u(x,0)$ with $\xi(0) = 0$, $\eta(0) = 1$, and $c = 1$ as ICs for a simulation, because Eq. (53) formally also holds for $\mu\lambda > 0$. Figure 2 shows a bisoliton, i.e., a bound state of two solitons. Their amplitudes, widths, and separation distance oscillate, while the norm and the energy are conserved.

Although our stability criteria Eqs. (3) and (4) were conjectured and confirmed only for single solitons, we can test whether the criteria also hold for the bisoliton in

Fig. 2. We must treat the solitons separately, which means that their positions $q(t) = N_1(t)/N$ and momenta $P(t)$ are defined by the integrals Eqs. (11) and (12) over $[0,\infty]$ for the right soliton and $[-\infty,0]$ for the left soliton, respectively. Although the oscillations of $P(t)$ and $q(t)$ are weakly anharmonic, the stability curve $p(v)$ is practically a straight line (Fig. 3). That is, the curvature is not visible because the asymmetry of each of the solitons is small.

V. PARAMETRICALLY DRIVEN SOLITONS OF THE CUBIC NLSE

In the Introduction, we reported four cases of NLSEs with nonparametric (external) driving. In all these cases, the driving term $R = a\exp(-iKx)$ on the right-hand side of the NLSE Eq. (1) does not vanish at infinity, thus the soliton solutions do not fulfill the vanishing boundary conditions that we have assumed in Sec. II. Therefore, Eq. (18) for $p(t)$ does not hold.

In the fifth case in the Introduction, the soliton is driven parametrically, i.e., the driving term on the right-hand side of Eq. (1) is chosen as

$$R = r\exp(2iKx)u^*(x,t), \tag{54}$$

with constant K. In this case, the soliton vanishes at the infinities and the vanishing boundary conditions of Sec. II are fulfilled, and therefore Eq. (18) holds.

Note that the appearance of the complex-conjugate field u^* in Eq. (54) is decisive: without the asterisk, we would have $R = V(x)u(x,t)$ and the soliton would move in the potential $V(x)$. This case has already been considered at the beginning of Sec. III.

For the parametrically driven soliton of the cubic NLSE, a CC theory has been developed [14] in which the $p(v)$ curve is calculated analytically. Depending on the IC, the soliton is predicted to be stable or unstable, and this is confirmed by simulations.

However, the CC theory is only an approximation, therefore our goal now is to calculate the $p(v)$ curve without using the collective variables. As an exact analytical solution for the parametrically driven soliton is not known, we work with the numerical solutions obtained by simulations for the NLSE Eq. (1) with the driving term Eq. (54).

As the IC we take the exact one-soliton solution of the unperturbed cubic NLSE in the representation of Ref. [12],

$$u(x,t) = 2i\eta\,\mathrm{sech}[2\eta(x-q)]e^{i[p(x-q)-\Phi]}. \tag{55}$$

To obtain the $p(v)$ curve, we have taken the following steps:

(i) For the integration of the NLSE, we use a fourth-order Runge-Kutta method and vanishing boundary conditions. The parameters related with the discretization of the system are $x \in [-100,100]$, $\Delta x = 0.05$; $\Delta t = 10^{-4}$ [such that the condition $\Delta t < (1/2)(\Delta x)^2$ is fulfilled].

(ii) From the simulation results, we compute the momentum P, the norm $N(t)$, and the first moment of the norm $N_1(t)$. The soliton position is $q(t) = N_1/N$ and the normalized momentum $p = P/N$.

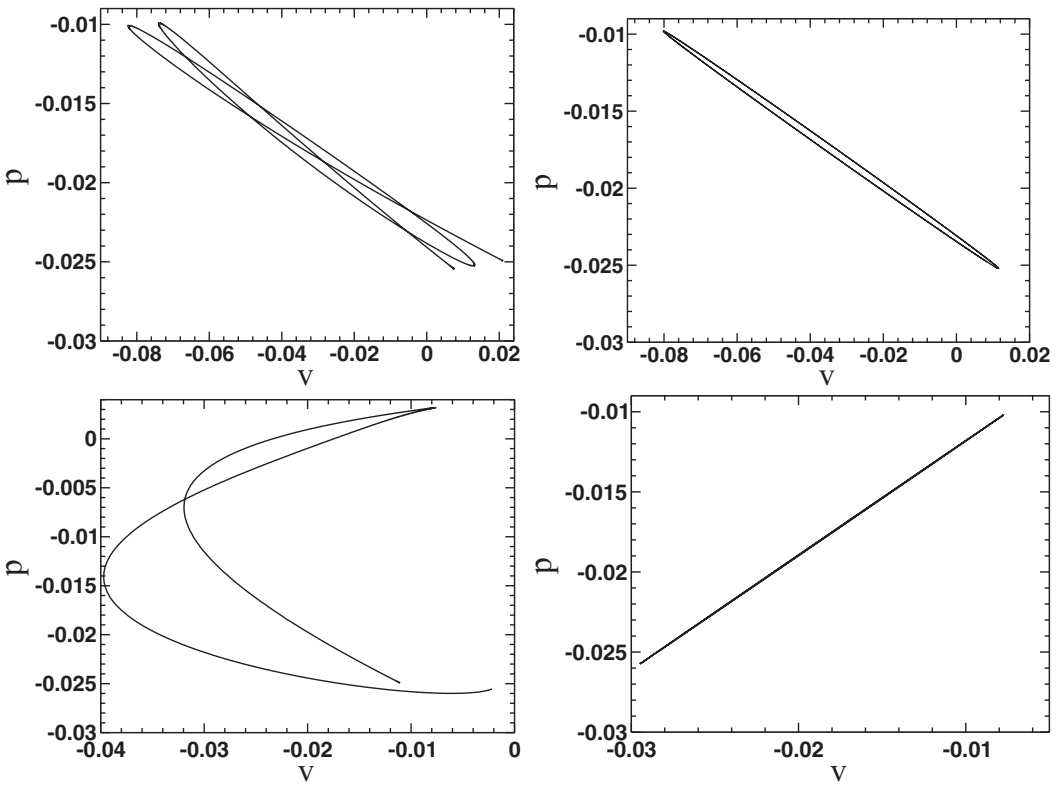

FIG. 4. Stability curves for parametrically driven solitons. IC: Eq. (55) with $\eta_0 = 0.25$ (upper left and right panels without and with the use of fitting functions, respectively), $\eta_0 = 0.35$ (lower left panel), $\eta_0 = 0.48$ (lower right panel). Other ICs: $q_0 = 0$, $\Phi_0 = \pi/2$, $p_0 = -K/4$. Parameters: $r = 0.05$, $K = -0.1$, $\delta = -1$.

(iii) The soliton velocity, $v = \dot{q}$, is obtained by a numerical differentiation using the five-point Lanczos method and a running average.

(iv) We observe that the functions $p(t)$ and $v(t)$ are nearly periodic. We compute their spectra by using the discrete Fourier transform (DFT). The spectra show essentially one peak at ω_1 or two peaks at ω_1 and $\omega_2 = 2\omega_1$.

(v) We fit the data from $p(t)$ and $v(t)$ in $t \in [0,2T]$, $T = 2\pi/\omega$, with the function $A_0 + A_1\cos(\omega_1 t + A_2) + A_3\cos(\omega_2 t + A_4)$, i.e., five fitting parameters for each of the functions. For the fitted functions used in Fig. 4, we obtain correlation coefficients between 0.97 and 0.998.

(vi) Using the fitting functions, we eliminate the time in $t \in [0,2T]$ and plot $p(v)$.

The upper panels in Fig. 4 demonstrate the effect of the fitting procedure by showing $p(v)$ curves with and without fitting. For the lower left panel, no fitting was used because here the functions $p(t)$ and $v(t)$ deviate too much from periodicity.

The $p(v)$ curves differ qualitatively, depending on the initial soliton amplitude. For small amplitude $\eta_0 = 0.25$, the slope $p'(v)$ is always negative (upper panels of Fig. 4), predicting instability. In our simulations, the average of the oscillating amplitude of the soliton decreases very slowly and the soliton vanishes asymptotically.

For intermediate values of the initial amplitude (e.g., $\eta_0 = 0.35$), the situation is completely different: there the $p(v)$ curve has two branches, one with positive and one with negative slope; in between, the slope has a singularity (lower left panel of Fig. 4). The lifetime of the soliton is short, suggesting that the soliton is destroyed by the changes between the positive and negative slope.

For larger initial amplitude (e.g., $\eta_0 = 0.48$) the $p(v)$ curve is a straight line with a positive slope (lower right panel of Fig. 4). This predicts stability of the soliton, which is confirmed by the simulations.

Finally, we want to discuss how Eq. (18) can yield a negative slope for the $p(v)$ curve. First of all, the second term in Eq. (18) vanishes because the profile $|u|^2$ of the soliton solution Eq. (55) is symmetric. The third term $F(t)$ vanishes if the soliton moves in a real potential (Sec. III). However, for the parametric drive, Eq. (54), $F(t)$ does *not* vanish because of the appearance of the complex-conjugate field $u^*(x,t)$. Depending on the values of the ICs, $F[t(\dot{q})]$ can be stronger than the first term $\dot{q}$ in Eq. (18) and then $p[\dot{q}]$ can have a negative slope.

VI. SUMMARY

In recent years, a stability criterion for the solitons of the driven NLSE was conjectured by us. A collective coordinate (CC) theory was used to calculate the so-called "stability curve" $p(v)$. The slope of this curve allowed us to make predictions about the soliton stability, and these predictions were confirmed by simulations.

The goal of this paper is to calculate the stability curve without using a CC theory because these theories are approximate. We have considered a generalized NLSE (GNLSE) with arbitrary nonlinearity and arbitrary driving, and we have derived an expression for $p(t)$ that contains two integrals that cannot generally be evaluated. Therefore, we have investigated several classes of GNLSE for which these integrals can be calculated exactly: We have considered a soliton moving in a real potential. In particular, we have calculated the $p(v)$ curve for the cases of a time-dependent ramp potential and a time-dependent confining quadratic potential, where the nonlinearity has a time-dependent coefficient. We also calculated the $p(v)$ curve for a logarithmic NLSE with a time-independent parabolic potential well. Here intrinsic anharmonic oscillations of the soliton width are coupled to the harmonic oscillations of the soliton position. For the cubic NLSE with a parabolic potential well there is a bisoliton, which consists of two solitons with asymmetric shapes. The solitons form a bound state in which the shapes and the separation distance oscillate. The $p(v)$ curve predicts stability, which is confirmed by numerical simulations. Finally, we have performed simulations for the cubic NLSE with parametric driving. The $p(v)$ curve is obtained numerically, and depending on the initial conditions, stability or instability is predicted and confirmed.

In the above GNLSE, the solitons vanish at the infinities. In the future, we plan to calculate the $p(v)$ curve for the case of nonvanishing boundary conditions. Moreover, we plan to consider the case of a symmetric soliton in a complex potential with an arbitrary real part and an even imaginary part.

ACKNOWLEDGMENTS

F.G.M. is grateful for the hospitality of the Mathematical Institute of the University of Seville (IMUS) and of the Theoretical Division and Center for Nonlinear Studies at Los Alamos National Laboratory, and financial support from the Plan Propio of the University of Seville, from Junta de Andalucia (Spain) IAC11-III-11965, and from the MICINN (Spain) through FIS2011-24540. N.R.Q. acknowledges financial support from the Alexander von Humboldt Foundation (Germany) through a Research Fellowship for Experienced Researchers SPA 1146358 STP and from the MICINN (Spain) through FIS2011-24540, and by Junta de Andalucia (Spain) under Projects No. FQM207, No. P11-FQM7276, and No. P09-FQM-4643. Work at Los Alamos is supported by the USDOE (USA).

[1] M. Vakhitov and A. Kolokolov, Radiophys. Quantum Electron. **16**, 783 (1973).
[2] M. I. Weinstein, Commun. Pure Appl. Math. **39**, 51 (1986).
[3] Y. Sivan, G. Fibich, B. Ilan, and M. I. Weinstein, Phys. Rev. E **78**, 046602 (2008).
[4] M. M. Bogdan, A. S. Kovalev, and A. M. Kosevich, Sov. J. Low Temp. Phys. **15**, 288 (1989).
[5] I. V. Barashenkov and E. Y. Panova, Physica D **69**, 114 (1993).
[6] D. E. Pelinovsky, Y. S. Kivshar, and V. V. Afanasjev, Phys. Rev. E **54**, 2015 (1996).

[7] I. V. Barashenkov, Phys. Rev. Lett. **77**, 1193 (1996).
[8] Z. Lin, Adv. Differential Equations **7**, 897 (2002).
[9] H. W. Schürmann and V. S. Serov, Phys. Rev. E **62**, 2821 (2000).
[10] I. V. Barashenkov, E. V. Zemlyanaya, and M. Bär, Phys. Rev. E **64**, 016603 (2001).
[11] F. G. Mertens, N. R. Quintero, and A. R. Bishop, Phys. Rev. E **81**, 016608 (2010).
[12] F. G. Mertens, N. R. Quintero, I. V. Barashenkov, and A. R. Bishop, Phys. Rev. E **84**, 026614 (2011).
[13] F. Cooper, A. Khare, N. R. Quintero, F. G. Mertens, and A. Saxena, Phys. Rev. E **85**, 046607 (2012).
[14] I. V. Barashenkov, F. G. Mertens, and N. R. Quintero (unpublished).
[15] H. H. Chen and C. S. Liu, Phys. Rev. Lett. **37**, 693 (1976).
[16] V. N. Serkin, A. Hasegawa, and T. L. Belyaeva, Phys. Rev. Lett. **98**, 074102 (2007).
[17] L. Wu, J. F. Zhang, and L. Li, New J. Phys. **9**, 69 (2007).
[18] M. de Moura, J. Phys. A **27**, 7157 (1994).
[19] R. Balakrishnan, Phys. Rev. A **32**, 1144 (1985).
[20] V. M. Pérez-García, P. J. Torres, and V. V. Konotop, Physica D **221**, 31 (2006).
[21] M. Gürses, arXiv:0704.2435.
[22] A. Kundu, Phys. Rev. E **79**, 015601 (2009).